International Conference on Control, Engineering & Information Technology (CEIT'13)
Proceedings Engineering & Technology - Vol.3, pp. 69-76, 2013

Geometric and Hemodynamic Study in Early Stages of Diabetic Retinopathy

Jihene Malek, Boutheina Nasralli, Fraj Echouchene, Rached Tourki
Electronics and Microelectronics Laborotory
Department of Physics
University of Monastir
jihenemalek@yahoo.fr

***Abstract*—The retinal microvasculature is a window to the systemic circulation. Systemic diseases, such as diabetes and hypertension, are associated with retinal microvascular structure (e.g., tortuosity, width and branching angle) changes; resulting in potentially disadvantageous blood flow. The purpose of this paper is to create a computational model of a retinal arterial network using computational fluid dynamics modeling (CFD, Fluent, ANSYS, Inc.). The CFD analysis will allow us to examine the effect of topological changes in retinal vasculature on hemodynamics distribution in the retinal circulation. This paper presents the results of a circulation analysis using 3 Fundus images for the same patient over times. The microvascular diameter effect (i.e., FahraeusLindqvist effect) and Hematocrit, were considered in determining the viscosity of the blood in the retinal vessel segments. A Comparison of relationship between change in the structure and his influence on blood flow are also presented. The method developed can be used as a tool for continuous monitoring of the retinal circulation for clinical assessments as well as experimental studies**

Keywords — Computational fluid dynamics, Hemodynamics, Fundus images, Finite-element method..

I. Introduction

The principal function of the microvasculature is transport of materials. Water and solutes are carried by blood through the microvessels and exchanged, through vessel walls, with the surrounding tissues. This transport function is highly dependent on the architecture of the microvasculature and on the biophysical behavior of blood flowing through it. Circulation analyses using a detailed image-based anatomical vascular of physiological systems have been proven useful in enhancing biologists' understanding of the hemodynamics of the system and thereby improve the treatment of circulation related diseases [1] [2] [3] [4] [5] [6] [7]. This is important since vascular circulation related diseases such as diabetes, hypertension and atherosclerosis are major health problems in modern society. Retina is the only tissue in which the blood vessel can be visualized non-invasively in vivo and this makes the study for retinal hemodynamics and blood flow regulation of special interest for both physiological and pathological conditions. In fact, fundus examination of retinal blood vessel and circulation not only plays an important role in the diagnosis of retinal diseases, but also provides valuable information for many of the aforementioned systemic vasculature related diseases. Structural changes in the microvasculature during the progression of diabetic retinopathy are well characterized. The challenge of ophthalmology management in patients with diabetes is the earliest detectable abnormalities in microvascular hemodynamics before gross morphologic changes appear; allowing the physician to intervene before complications arise and the effects of the disease become irreversible. Therefore, being able to construct a model based on measured geometry will enable us to quantitatively understand the hemodynamics in a realistic retinal vascular network. Computed pressure and flow profiles could be very useful tool to diagnose arterial or venous disease. For a given subject, measured pathologic flow profiles could be compared with computed healthy flow profiles. Studies of how the model parameters must change to simulate the measured pathologic flow profiles might lead to a better understanding of the pathologic condition.

The goal of this work is to develop and use a one dimensional fluid-dynamical model predicting blood flow and pressure in the human retinal arterial network at any position along the vessels. Such a model can be used to study the profile of the flow and pressure waves as they propagate along the arteries. The form of the waves change as a result of the arteries changing geometry and structure [8] [9]. Although there are many modeling studies on blood flow in large arteries, [10] [11] [12] [13] little work has been done on the retinal microcirculation [14] [15].

In the present study, a detailed 2-D computational model was developed to simulate blood flow in a realistic retinal arterial tree by solving Navier-Stokes equations. The geometrical outlines of the central retinal artery and its major branches were obtained from retinal images captured by a fundus camera. Smaller peripheral vessels indistinguishable from the images were represented by a structured tree generated at each of the outlets in the reconstructed network to model the heterogeneous anatomy of the downstream vascular bed, and equal exit pressures were assumed at the terminals of this virtual extended network. Because of the small dimensions of the retinal circulation, it was considered desirable to implement in the flow simulation an empirical non-Newtonian viscosity model of blood incorporating the Fahraeus-Lindqvist effect [16]. Numerical analysis of blood flow in retinal vascular trees in early stages of diabetic retinopathy was performed.

One of the first changes in vessel morphology to occur is

the increase in vessel tortuosity. The clinical recognition of abnormal vascular tortuosity is important in the diagnosis of many diseases. In order to evaluate the clinical significance of tortuosity changes with time, and to compare different levels of the same retinopathy a number of tortuosity measures have been proposed [17][18][19][20]. Variations in blood vessel diameters occur as part of the autonomous control of blood flow in healthy subjects and at different stages in the pulse cycle [21], while sustained changes may also indicate the presence of some pathology [22]. Measurements of vessel width are therefore of interest both to physiologists looking to better understand the regulation of blood flow [23] [24] and to clinicians interested in the prediction, diagnosis or progression of disease [25] [26] [27]. However, an accurate measurement is complicated, because of the large variation in fundus images. Especially for small vessel branches, an accurate measurement can be complicated because of noise and the low vessel contrast. Blood vessels are segmented using two-dimensional matched filters, which involves filtering the image with a family of 1D filters derived from Gaussian functions (chosen to model the profile across most vessels) rotated at different angles, then retaining the largest magnitude response [28], This segmentation provided measurement of vessel widths and tortuosity.

II. Characterization of Changes in Blood Vessel Width and Tortuosity in Retinopathy Using Image Analysis

Many retinal diseases are characterized by changes to retinal vessels. Normal retinal blood vessels are straight or gently curved. In some diseases, the blood vessels become tortuous, i.e. they become dilated and take on a serpentine path. The dilation is caused by radial stretching of the blood vessel and the serpentine path occurs because of longitudinal stretching. Automatic measurement of blood vessel tortuosity is a useful capability for automatic ophthalmological diagnostic tools. Information about disease severity or change of disease with time may be inferred by measuring the tortuosity of the blood vessel network. Consequently, there is a benefit in measuring tortuosity in a consistent, repeatable fashion. We describe a suite of automated tortuosity measures for blood vessel segments extracted from RGB retinal images.

A. Preprocessing

We have used 4 serial images were collected from retinopathy patient. To extract blood vessel segments, we applied the blood vessel filter described in [28] to the green plane of an RGB image; the green plane was selected because it typically exhibits the greatest contrast. The filter was applied at 12 orientations over 180^o. The final response map was computed by taking the maximum response of the 12 filters at each location. The skeletons of the segmented trees are produced by a thinning technique, branching and crossing points are identified and segments of the trees are labelled and stored as a chain code. Fig.1a show original image and Fig.1b show the skeleton lines and the significant points over imposed in the original image.
Skeletonisation allows identification of points in the image where vessels cross (bifurcations, crossing points and endpoints) and allows the width and tortuosity of vessel segments to be calculated.

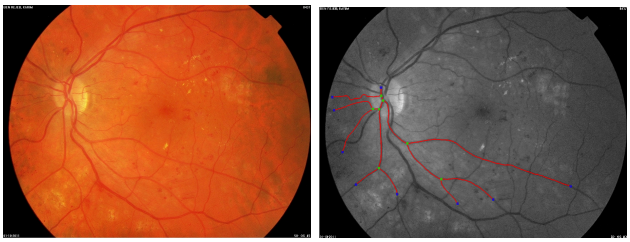

(a) (b)

Figure 1. Process to extract a tree from binary image. (a) RGB fundus image (b) show skeleton and significant points marked over the original image

B. Vessel Tortuosity Calculation

The tortuosity may be focal; occurring only in a small region of retinal blood vessels, or it may involve the entire retinal vascular tree. Fig.2 shows images with tortuous and non-tortuous blood vessels.

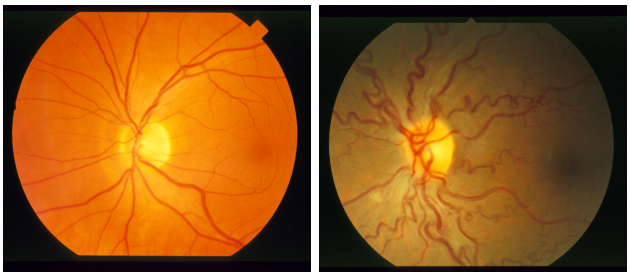

(a) (b)

Figure 2. Images with (a) tortuous and (b) non-tortuous blood vessel segments.

The tortuosity is trivial to calculate once the constituent points of the vessel segment have been recorded in their own data structure. The distance traversed by the vessel is calculated by summing the distance between consecutive points in the segment:

$$d_{curve} = \sum_{i=1}^{N-1} \sqrt{(x_{i+1} - x_i)^2 + (y_{i+1} - y_i)^2} \qquad (1)$$

Where (xi, yi) are the co-ordinates of the ith pixel in the vessel segment, and the vessel segment has N constituent points. The straight distance is calculated as the distance between the first and last points of the vessel :

$$d_{straight} = \sqrt{(x_N - x_1)^2 + (y_N - y_1)^2} \quad (2)$$

The tortuosity of a vessel segment is defined as the ratio of the curved distance and the straight distance:

$$Tortuosity = \frac{d_{curve}}{d_{straight}} \quad (3)$$

Measure of tortuosity requires a segmentation of vessels Fig.3a. Then partition these vessels in the vessel segments. Finally, calculation the ratio of the curved distance and the straight distance Fig.3b for each segment.

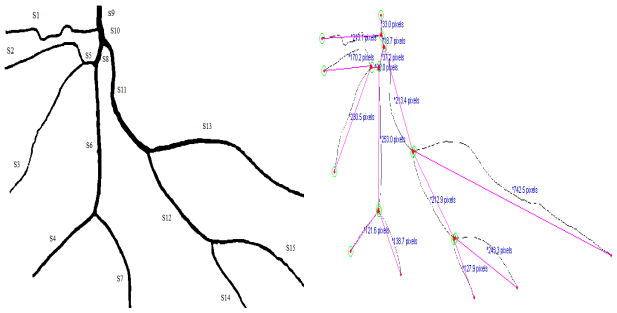

(a) (b)

Figure 3. Arterial trees were identified by an operator (a).The tortuosity measure of each segment (b).

The same steps as previously described are applied for four fundus images for the same patient and taken in different dates over 18 months. Each vessel segment has its own vessel tortuosity which varies from one image to other. This value changes from one examination to another depending on the stage of the disease. Normal values of tortuosity not exceeding 1.1 and 1.2 maximum, otherwise disease is serious and direct effects blood vessel. The treatment given to the patient may improve vessel tortuosity over time as seen in Table I.

TABLE I
CHANGES IN VESSEL TORTUOSITY OVER TIME FOR RETINOPATHY PATIENT

Segment	09−04−2010	30−10−2010	01−10−2011
S1	1.17	1.16	1.14
S2	1.22	1.22	1.21
S3	1.11	1.09	1.09
S4	1.06	1.08	1.06
S5	1.02	1.02	1.04
S6	1.04	1.04	1.04
S7	1.10	1.09	1.08
S8	1.08	1.08	1.08
S9	1.07	1.07	1.04
S10	1.08	1.08	1.07
S11	1.15	1.13	1.14
S12	1.08	1.09	1.10
S13	1.09	1.09	1.10
S14	1.07	1.08	1.07
S15	1.11	1.10	1.11

C. Calculation of vessel Width

Accurate determination of retinal vessel width measurement is important in the study of the hemodynamic changes that accompany various physiological and pathological states. The next step is to find the width at every point in the vessel segment. For this project, for each point M on the central line, the orientation D orthogonal to the axis of a potential vessel that goes through M is defined. From this direction, a line segment is extended from both sides of a pixel in the mask image simultaneously until a imbackground (0) pixels is met (M1, M2). The distance can be measured, as the length of the line segment [M1 M2] (Fig. 4a).

The width at every point in the vessel segment was computed using this method (Fig. 4b).

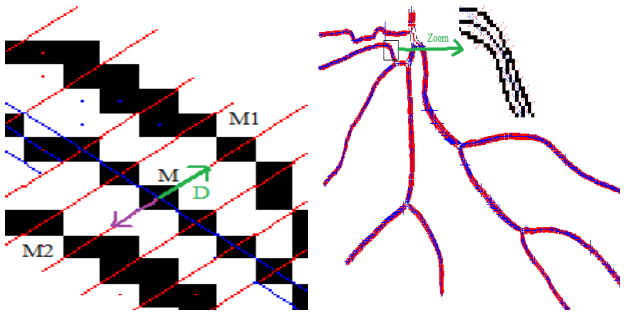

(a) (b)

Figure 4. Illustration of the vessel width calculation. From the point M on the central line, D is the unit vector perpendicular to the main direction of the vessel (a).The width calculation of the tree with Subimage for better visualization(b).

An average vessel width of each section of the segmented retinal arteries were calculated (see Table II)

TABLE II
CHANGES IN VESSEL WIDTH OVER TIME FOR RETINOPATHY PATIENT

Segment	09−04−2010	30−10−2010	01−10−2011
	Computed width (μm)	Computed width (μm)	Computed width (μm)
S1	38.9772	43.464	35.184
S2	38.124	36.636	36.672
S3	44.052	40.512	31.656
S4	47.52	49.584	46.5
S5	29.436	31.716	27.252
S6	54.312	54.636	53.232
S7	46.224	45.384	45.816
S8	41.052	42.672	40.86
S9	96.168	90.444	79.272
S10	94.884	90.852	88.86
S11	69.36	61.62	61.44
S12	49.104	48.852	48.768
S13	52.8	49.428	46.992
S14	39.996	37.512	35.88
S15	47.316	47.028	42.54

Pathogenetic changes in retinal microvessel structure as

diabetic retinopathy is a major cause of structural changes Structural changes were accompanied by a decrease in retinal blood flow

III. Retinal Blood Flow Simulation

A. Flow Model

This paper presents a mathematical modeling of the arterial blood flow which was derived from the Navier-Stokes equations and some assumptions for incompressible flow.

$$\nabla.\overrightarrow{V} = 0 \tag{4}$$

$$\rho\left(\overrightarrow{V}.\nabla\right)\overrightarrow{V} = -\nabla p + \mu\nabla^2\overrightarrow{V} \tag{5}$$

Where $\overrightarrow{V}$ is the blood velocity, p is the pressure, and ρ and μ refer to the density and dynamic viscosity of blood, respectively. It is known from previous studies that the circulation in microvasculature, especially in those of a diameter $< 100\,\mu m$, can be significantly affected by the non-Newtonian rheological properties of blood. This is due to the comparable length scale of the vessel diameter and blood cells. Red blood cells (RBCs) which have a larger fraction than other blood cells are found to play a huge role in determining the viscosity of the blood. Blood hematocrit, which influences blood viscosity, is defined by the ratio of RBCs volume over the total blood volume. Since the diameters of the retinal arteries are less than $< 100\,\mu m$, the assumption of blood as an ideal homogenous Newtonian fluid would be invalid owing to the complex characteristics of blood, and its particulate nature has to be considered. In microcirculation, the apparent viscosity of blood depends on hematocrit and vessel diameter, known as the Fahraeus-Lindqvist effect. The FahraeusLindqvist effect, which was first observed by Martini et al. [29] and Fahraeus and Lindqvist [30], refers to the reduction of the apparent viscosity of the blood with decreasing tube diameter as diameter $< 500\mu m$. Apparent viscosity of a non-Newtonian fluid stands for the viscosity of a Newtonian fluid that would give the same volume flow rate for a given tube geometry and driving pressure. To account for this effect, the empirical viscosity model proposed by Pries et al.[31] was adopted.

$$\mu_{rel}\left(D, H_D\right) = \left[1 + \left(\mu_{0.45} - 1\right).\frac{\left(1-H_D\right)^C - 1}{\left(1-0.45\right)^C - 1}.\left(\frac{D}{D-1.1}\right)^2\right].\left(\frac{D}{D-1.1}\right)^2 \tag{6}$$

Here $\mu_{0.45}$, the relative blood viscosity for a fixed discharge hematocrit of 0.45, is given by

$$\mu_{0.45} = 6e^{-0.085D} + 3.2 - 2.44e^{-0.06D^{0.645}} \tag{7}$$

D is the vessel diameter, and C describes the shape of viscosity depen- dence on hematocrit.

$$C = \left(0.8 + e^{-0.075D}\right).\left(-1 + \frac{1}{1+10^{-11}.D^{12}}\right) + \frac{1}{1+10^{-11}.D^{12}} \tag{8}$$

Due to disproportionate distribution of red blood cells and plasma at bifurcations, hematocrit has been reported to vary with radius in small vessels [16]. In this study, a constant hematocrit of 0.45 was assumes [32]. Blood flow was assumed to be incompressible flow and has been steady and governed by the Navier-Stokes equations. The density of blood was assumed to be 1050 kg/m3 and the walls were considered rigid.

B. Impedance Boundary Condition for Vascular Networks

The resistance to blood flow through a vascular network define the vascular impedance. Impedance used as an outlet boundary condition. It can be computed from the structured trees that represent vascular beds. In [5] Olufsen *et al* computed impedance from linear, axisymmetric, 1D equations for conservation of mass and momentum. Along each vessel in the structured tree, the input impedance is computed at the beginning of each vessel $Z = 0$ as a function of the impedance at the end of a vessel $z = L$ (Fig. 5):

$$Z\left(0,\omega\right) = \frac{ig^{-1}\sin\left(\omega L/C\right) + Z\left(L,\omega\right)\cos\left(\omega L/C\right)}{\cos\left(\omega L/C\right) + igZ\left(L,\omega\right)\sin\left(\omega L/C\right)} \tag{9}$$

L is vessel length, $c = \sqrt{s_0\left(1 - F_J\right)/\left(\rho C\right)}$ is the wave-propagation velocity, where:

$$Z\left(0,0\right) = \lim_{\omega\to 0} Z\left(0,\omega\right) = \frac{8\mu l_{rr}}{\pi r_0^3} + Z\left(L,0\right)\; F_J = \frac{2J_1\left(\omega_0\right)}{\omega_m J_0\left(\omega_0\right)} \tag{10}$$

$J_0\left(x\right)$ and $J_1\left(x\right)$ are the zero'th and first order Bessel functions with $\omega_0^2 = i^3 w$ and $\omega^2 = r_0^2\omega/v$. The compilance C is approximated as :

$$C \approx \frac{3s_0 r_0}{2Eh} \tag{11}$$

where, s_0 is the reference cross-sectional area and $l_{rr} = L/r$ is the length-to-radius ratio.

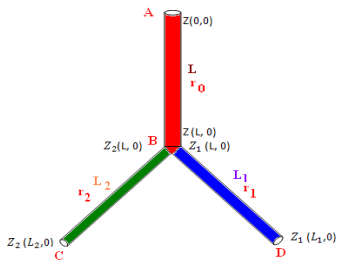

Figure 5. An arterial tree with three branches..

C. The geometry of the structured tree

Due to the limited resolution of the fundus camera and the heterogeneous peripheral vascular bed, smaller arterioles were unresolved. Hence,the arteriolar network was truncated asymmetric structured fractal trees with self-similar binary bifurcations were generated at each of the visible network outlets (Fig. 6)[11] [12].

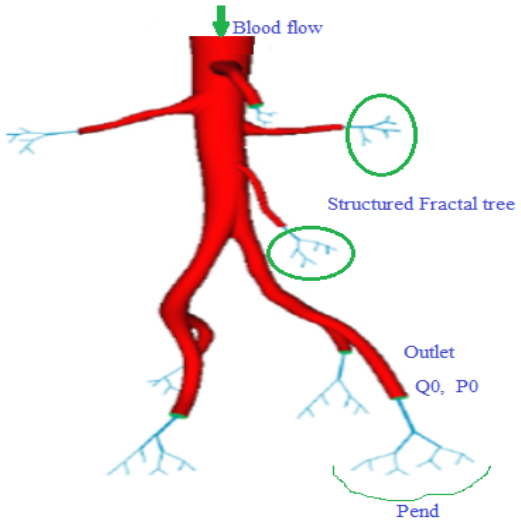

Figure 6. Schematic structured fractal tree

The branching relationship across bifurcations between the radius of the parent vessel r_p and the radii of the daughter vessels $r_{di}(i = 1, 2)$, can be described as :

$$r_p^{\xi} = r_{d1}^{\xi} + r_{d2}^{\xi},\ \gamma = \frac{r_{d1}}{r_{d2}} \tag{12}$$

If $\xi = 2$, then area will be conserved. Murray [33] derived that maximum efficiency for blood flow is attained when $\xi = 3$. Other observation has been suggested that k may vary depending on the radius of the branches involved. Many studies show that k varies from 2 to 3 with mean values given by 2.5, 2.7 and 2.9 ([34] ;[35];[36]). γ, is known as the asymmetry ratio. The asymmetry index describes the relative relationship between the daughter vessels. Finally, the length of a given artery (between bifurcations) can be expressed as a function of the mean radius of the vessel. Based on the analysis of retinal vascular morphology by Martinez-Perez [37] and [38] values for the asymmetry ratio and length to radius ratio l_{rr} were derived and shown in Table III

The properties described above are originally used by Olufsen [11].In the tree, the radii of successive daughter vessels (r_{d1} and r_{d2}) were obtained by introduction of scaling parameters α and β for the radius of the root vessel (r_{root}) such that:

$$r_{d1} = \alpha r_{root},\ r_{d2} = \beta r_{root}\ and\, r_{i,j} = \alpha^i \beta^{j-i} r_{root} \tag{13}$$

and

$$\alpha = \left(1 + \gamma^{k/2}\right)^{-(1/k)}\ and\ \beta = \alpha\sqrt{\gamma} \tag{14}$$

In our implementation of the structured tree, the Table III were developed based on the literature described above and these parameters has been reported in [14]. Here, we assumed that retinal arterioles with outlets smaller than 15 μm in radius where pressure is set to be 0.0 mmHg. Therefore, all the outlets in the visible tree with radius greater than 15 μm were connected to an asymmetric structured tree generated for each outlet to represent its downstream vascular bed. The fractal tree extended until the mean radius of the major daughter vessel r_{d2} was less than 15 μm. Pressure derived from the total resistance of the fractal tree and corresponding volumetric flow, was specifed as outfow boundary condition at each outlet Fig. 6.

TABLE III
GEOMETRY PARAMETERS FOR THE FRACTAL TREE MODEL

Range	γ	ξ	l_{rr}
$r < 22\mu m$	0.78	3	27
$r > 22\mu m$	0.64	3	29

IV. RESULTS END DISCUSSION

A. Healthy retina

The average radius and length of each section of the segmented retinal arteries were calculated. The Cartesian coordinates of the segmented vessels and skeletons were determined via a Matlab program and were imported into Gambit 2.3. and then meshed for CFD simulation. Image scale was estimated on the basis of a standard disc diameter (assumed to be 1850 μm) [39]. Due to the limited resolution of the fundus camera, the retinal arterial network obtained only includes arteries greater than $30\mu m$, and more peripheral vessels were unresolved.

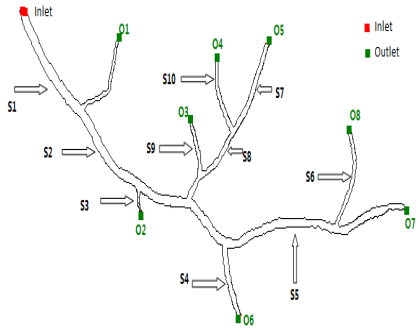

Figure 7. An arterial tree.

The Reynolds-averaged Navier-Stokes equations were solved numerically via the commercial finite volume CFD solver, Fluent 6.3, supplemented by the fractal tree model at model outlets, the Pries model for blood viscosity. A uniform velocity ($\overrightarrow{V}$) from the central retinal artery of 0.07 m/s [40]

was specified at the inlet. The inlet velocity profile was set to be uniform across the lumen, but due to the low Reynolds numbers fully-developed profiles could be rapidly established. The outline of the image-based retinal arteriolar network is shown in Fig. 7. For this visible network, there are 8 outlets represented by Oi (i =1 to 8), respectively. The segments of the retinal arterioles are described as Si (i = 0 to 10).

The retinal vascular network constitutes a complex geometry. Given this difficulty, in our work we use and hybrid mesh Fig. 8.

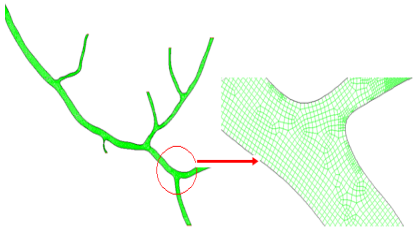

Figure 8. Discretized structure.

Fig. 9 shows the blood flow distributions in the retinal arterial network. The velocity field varies between a minimum value close to the wall and a maximum value at the center of the flow. Maximum value is on average 0.18 m/s. We note that the blood flow reach slowly the outlets. This is due to the slow rate of injection and the bifurcation of the vessel which makes the friction important.

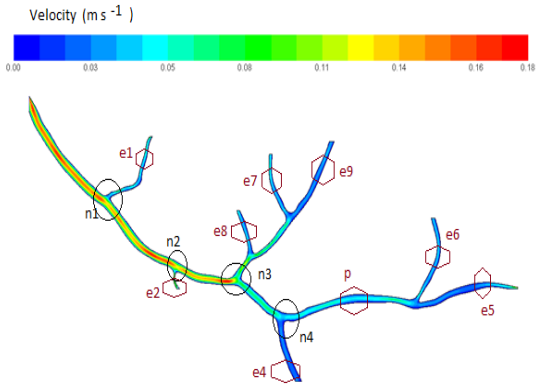

Figure 9. Computational Velocity Results.

Fig. 10 shows the velocity profiles at different sections . The distribution of blood flow in the retinal circulation depends on the geometry of the reconstructed vascular network as well as peripheral resistances at the model outlets. Owing to the low Reynolds number, a fairly uniform flow pattern was obtained in each arterial segment. Velocity profiles were close to parabolic in the parent vessel and main branch, but become flatter further downstream. The very low rate of blood flow in the arterioles provides sufficient time to carry out exchanges with tissue cells.

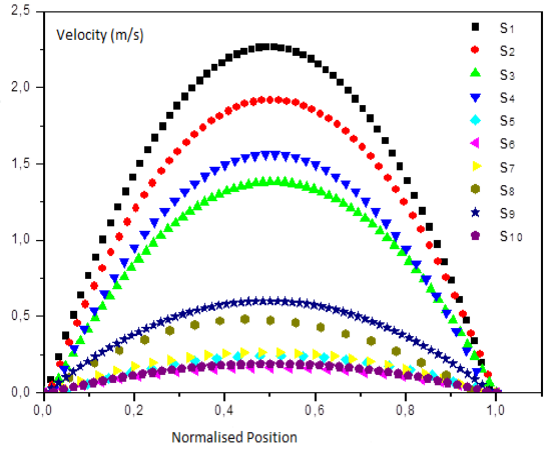

Figure 10. Velocity profiles at different sections in the left main branch of retinal arterial tree.

The velocity field of a flow is given by :

$$U = U_{max}\left(1 - \left(\frac{r}{R}\right)^2\right) \tag{15}$$

Where U_{max} is the maximum velocity of the blood in each section, and R is the radius of the vessel (either parent or child).

B. *diabetic retinopathy*

In order to study the evolution of the disease for a diabetic patient, we will use 3 fundus images over two years.

Retinopathy is characterized by the increase in blood viscosity due to hyperglycemia. The friction of the blood with the arteries walls slowing blood flow and consequently decreasing speed. We note that the velocity of blood decreases with the progression of the disease. Indeed, the simulation of blood flow gives an average value of blood velocity in the range of 0.052 m / s in the first case and then it decreases to a value of 0.04 m / s in the third case Fig. 11.

Arteries are conduits through which blood is pumped from the heart to organs,but in addition they have a smoothing function where large changes in blood pressure and flow resulting from intermittent ventricular ejection are integrated into a more steady flow within peripheral tissues. The most effective factor for controlling the blood flow is the radius of the blood vessel.

V. Conclusion

The study yielded detailed distributions of the hemodynamic quantities in the retinal arterial trees based contour plots. Quantitative analysis was also carried out based on CFD analysis. The peripheral Circulation was incorporated by using a structured fractal tree model to provide outlet boundary conditions. Numerical analysis of blood flow in retinal vascular trees in early stages of diabetic retinopathy was performed.The results presented can be directly useful to ophthalmologists and researchers working with retinal vasculature.

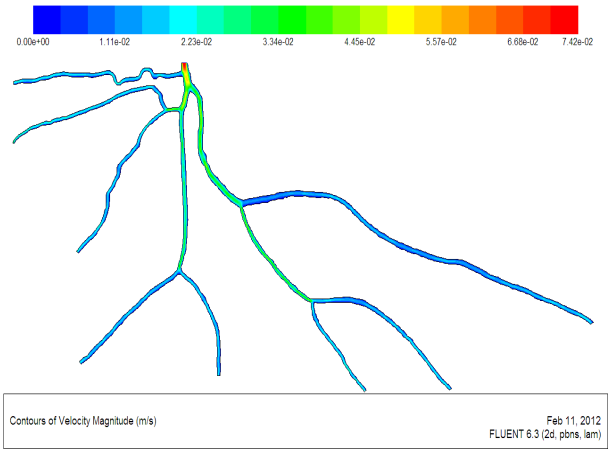

(a)

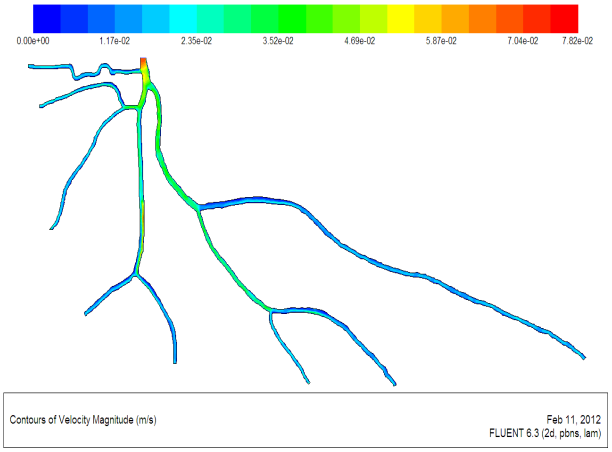

(b)

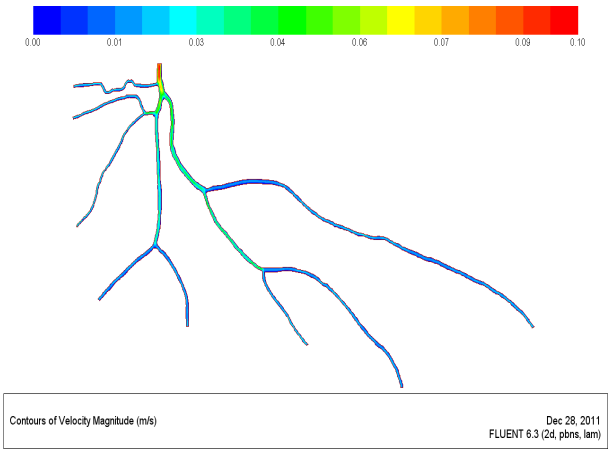

(c)

Figure 11. Velocity profiles at different sections in diabetic retinopathy arterial tree (a)diabetic 1 (b)diabetic 2 (c) diabetic 3

REFERENCES

[1] J. Lee, S. Nellis, Modelling study on the distribution of flow and volume in the microcirculation of cat mesentery, Ann. Biomed. Eng. 2, pp. 206-216, 1974.

[2] H. Lipowsky, B. Zweifach, Network analysis of microcirculation of cat mesentery, Microvas. Res. 7, pp.73-83, 1974.

[3] H. Lipowsky, S. Kovalcheck, B. Zweifach, The distribution of blood rheological parameters in the microvasculature of cat mesentery, Circ. Res. 43, pp. 738-749, 1978.

[4] G.Kassab, J.Berkley, Y.Fung , Analysis of pig's coronary arterial blood flow with detailed anatomical data, Ann. Biomed. Eng. 25, pp.204-217, 1997.

[5] M. Olufsen, C.Peskin, W. Kim, E. Pedersen, A. Nadim, , Larsen, J. Numerical simulation and experimental validation of blood flow in arteries with structuredtree outflow conditions. Ann.Biomed. Eng. 28, 1281-1299, 2000.

[6] Mittal, N., Zhou, Y., Linares, C., Ung, S., Kaimovitz, B., Molloi, S., Kassab, G. Analysis of blood flow in the entire coronary arterial tree. Am. J. Physiol. (Heart Circ. Physiol.) 289, H439-H446, 2005.

[7] J. Yang, L. X. Yu, M. Y. Rennie, J. G. Sled, and R. M. Henkelman1,2. Comparative structural and hemodynamic analysis of vascular trees. .Am J Physiol Heart Circ Physiol 298: .249-259,2010.

[8] Nichols, W. W., and M. F. ORourke. McDonalds Blood Flow in Arteries, 4th ed. London: Edward Arnold, , p.564, 1998.

[9] Peskin, C. S. Partial Differential Equations in Biology. NewYork: Courant Institute of Mathematical Sciences, New York University, pp. 160208, 1976.

[10] Sun N, Wood NB, Hughes AD, Thom S, Xu XY. Fluid-wall modelling of mass transfer in an axisymmetric stenosis: Effects of shear-dependent transport properties. Ann Biomed Eng. 34: 1119-1128, 2006

[11] Olufsen MS. A structured tree outflow condition for blood flow in the larger systemic arteries. Am J Physiol. 1999;276:H257-H268.

[12] Steele BN, Olufsen MS, Taylor C. Fractal network model for simulating abdominal and lower extremity blood flow during resting and exercise conditions. Computer Methods in Biomech and Biomed Eng. 2007;10:39-51.

[13] David A. Steinman. Image-Based Computational fluid dynamics modeling in realistic arterial geometries. Annals of Biomedical Engineering, Vol. 30, pp. 483-497, 2002

[14] D. Liu; N. B. Wood; N. Witt; A. D. Hughes; S. A. Thom; X. Y. Xu. Computational analysis of oxygen transport in the retinal arterial network. Current Eye Research, 34(11), 945-956, 2009

[15] P. Ganesan, S. He, H. Xu. Analysis of retinal circulation using an image-based network model of retinal vasculature. Microvascular Research 80 99-109, 2010

[16] Pries AR, Secomb TW, Gaehtgens P, Gross JF. Blood flow in microvascular networksexperiments and simulation.Circ Res.67:826-834. 1990

[17] . E. Bullitt, G. Gerig, S. Pizer et al. Measuring tortuosity of the intracerebral vasculature from mra images. IEEE Trans. Med. Img. 22, pp. 1163-1171, 2003.

[18] C. Heneghan, J. Flynn, M. OKeefe et al. Characterization of changes in blood vessel width and tortuosity in retinopathy of prematurity using image analysis. Med. Img. Analys. 6, pp. 407-429, 2002.

[19] W. Hart, M. Goldbaum, B. Cote et al. Measurement and classification of retinal vascular tortuosity. Int. Journ. Medical Informatics 53, pp. 239-252, 1999.

[20] E. Grisan, M. Foracchia , A. Ruggeri,A novel method for the automatic evaluation of retinal vessel tortuosity, Proc. 25th IEEE EMBS pp. 866-869, 2003.

[21] Knudtson MD, Klein BEK, Klein R, Wong TY, Hubbard LD, et al. Variation associated with measurement of retinal vessel diameters at different points in the pulse cycle. Br J Ophthalmol 88: 57-61, 2004.

[22] Patton N, Aslam TM, MacGillivray T, Deary IJ, Dhillon B, et al. Retinal image analysis: concepts, applications and potential. Prog Retin Eye Res 25:99-127, 2006.

[23] Fischer JG, Mewes H, Hopp HH, Schubert R, Analysis of pressurized resistance vessel diameter changes with a low cost digital image processing device,. Comput Meth Prog Bio 50: 23-30, 1996.

[24] Tyml K, Anderson D, Lidington D, Ladak HM, A new method for assessing arteriolar diameter and hemodynamic resistance using image analysis of vessel lumen,. Am J Physiol Heart Circ Physiol 284: H1721-8, 2003.

[25] Patton N, Aslam T, Macgillivray T, Pattie A, Deary IJ, Retinal vascular image analysis as a potential screening tool for cerebrovascular disease: a rationale based on homology between cerebral and retinal microvasculatures. J Anat 206: 319-348, 2005.

[26] Sun C, Wang JJ, Mackey DA, Wong TY, Retinal vascular caliber: Systemic, environmental, and genetic associations. Surv Ophthalmol 54: 74-95, 2009.
[27] . Wang JJ, Liew G, Klein R, Rochtchina E, Knudtson MD,Retinal vessel diameter and cardiovascular mortality: pooled data analysis from two older populations. Eur Heart J 28: 1984-1992, 2007.
[28] S. Chaudhuri, S. Chatterjee, N. Katz, M. Nelson et M. Goldbaum. Detection of blood vessels in retinal images using two-dimensional matched filters, IEEE Transaction on Medical Imaging, 8(3): 263-269, Septembre 1989.
[29] Martini, P., Pierach, A., Schreyer, E.,. Die stromung des blutes in eigen gefassen. eine abweichung vom poiseuilleschne gesetz. Dtsch. Arch. Klin. Med. 169, 212-222, 1930
[30] Fahraeus, R., Lindqvist, T., The viscosity of the blood in narrow capillary tubes. Am. J. Physiol. 96, 562-568, 1931.
[31] Pries AR, Secomb TW, Gaehtgens P. Biophysical aspects of blood flow in the microvasculature. Cardiovascu Res.32:654-667, 1996
[32] Iftimia NV, Hammer DX, Bigelow CE, Rosen DI, Ustun T, Ferrante AA, Vu D, Ferguson RD. Toward noninvasive measurement of blood hematocrit using spectral domain low coherence interferometry and retinal tracking. Optics Express.14:3377-3388,2006.
[33] C.D. Murray, The physiological principle of minimum work. I. The vascular system and the cost of blood volume, Proc. Natl. Acad. Sci. USA, 12, pp. 207-214, 1926.
[34] A.S. Iberall, Anatomy and steady flow characteristics of the arterial system with an introduction to its pulsatile characteristics, Math. Biosci., 1, pp. 375-395, 1967.
[35] M. Zamir, On fractal properties of arterial trees, J. Theor. Biol., 197, pp. 517-526, 1999.
[36] R. Karch, F. Neumann, M. Neumann andW. Schreiner, Staged growth of optimized arterial model trees, Ann. Biomed. Eng., 28, pp. 495511, 2000.
[37] Martinez-Perez ME. Computer Analysis of the Geometry of the Retinal Vasculature. PhD thesis, Imperial College London; 2000.
[38] Zamir M, Medeiros JA. Arterial branching in man and monkey. J Gen Physiol. 79:353-360, 1982.
[39] Hubbard LD, Brothers RJ, King WN, Methods for evaluation of retinal microvascular abnormalities associated with hypertension/sclerosis in the atherosclerosis risk in communities study. Ophthalmology 106:2269-2280, 1999.
[40] Evans DW, Harris A, Danis RP,. Altered retrobulbar vascular reactivity in early diabetic retinopathy. Br J Ophthalmol 81: 279-282, 1997.